Hyperelastic modelling of rubber with multi-walled carbon nanotubes subjected to tensile loading

M.J. Jweeg [a], D.A. Alazawi [b], Q.H. Jebur [c], M. Al-Waily [d],*, N.J. Yasin [e]

[a] College of Technical Engineering, Al-Farahidi University, Iraq
[b] Department of Mechanical Engineering, College of Engineering, University of Diyala, Iraq
[c] Climate Change-Scotland, UK
[d] Department of Mechanical Engineering, Faculty of Engineering, University of Kufa, Iraq
[e] Engineering Technical College of Baghdad, Middle Technical University, Iraq
* Corresponding e-mail address: muhanedl.alwaeli@uokufa.edu.iq
ORCID identifier: ⓘhttps://orcid.org/0000-0002-7630-1980 (M.A.-W.)

ABSTRACT

Purpose: This study thoroughly examined the application of inverse FE modelling and indentation tensile tests to identify nanotubes' rubber material properties.

Design/methodology/approach: Carbon nanotubes with various percentages of multi-walled carbon nanotubes exposed to high tensile stress were used to enhance the mechanical qualities of N.R. rubber.

Findings: In this work, carbon nanotubes have been added to natural rubber. By using a solvent casting technique, toluene was used to make nanocomposites. 0.2%, 0.4%, 0.6%, 0.8%, and 1%. In this article, rubber and multi-walled carbon nanotubes interact in practical ways. Mechanical features of carbon nanotubes in NR have been researched. The results will lead to rubber products with improved mechanical qualities compared to present nanocomposite rubber containing various percentages of multi-walled carbon nanotubes exposed to large tensile test loading. The relative fitness error for significant stresses is reasonable with a second or third-order deformation model in numerical results.

Research limitations/implications: Non-linear finite element analysis is widely used to optimise complicated elastomeric components' design and reliability studies. However, accurate numerical results cannot be achieved without using rubber or rubber nanocomposite materials with reliable strain energy functions.

Practical implications: The indentation tensile tests of rubber samples have been simulated and confirmed using a parametric FE model. An inverse materials parameter identification algorithm was used to calculate the hyperelastic material properties of rubber samples evaluated in uniaxial tensile. Using ABAQUS FE software, material parameters and force-displacement data may be automatically updated and extracted.

Originality/value: The numerical data for the inverse method of material property prediction has been successfully established by developing simulation spaces for various material characteristics. The force-displacement curve can be represented using technical methods. The results demonstrate that the inverse FE modelling process might be simplified by using these curve fitting parameters and plot equations to build a mathematical link between curve
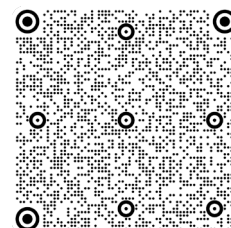
coefficients and material properties. The first, second, and third-order deformation models were tested using FE simulations for the tensile test.

METHODOLOGY OF RESEARCH, ANALYSIS AND MODELLING

1. Introduction

Rubber and rubber-like materials display many unique physical and chemical characteristics, including elasticity, resilience, flexibility, shock absorption, damping, sealing capabilities, and insulation, among other materials [1,2]. These qualities allow the rubber to be used in many industrial and technical applications [3,4], including tyres, hoses, conveyor belts, seals, damping components, and artificial soft tissue. Rubber's stress-strain response is a critical research area. Finite element analysis (FEA) has been effectively applied to structural optimisation and reliability analysis of complex rubber components with substantial deformation thanks to rapid advancements in computer power and non-linear numerical simulation techniques [5-7].

Similarly, polymer composites have been quite significant in manufacturing tires. Fillers nanocomposites are often used as additives to enhance the mechanical behaviour of the polymeric matrix. Reinforcing elastomers with mineral fillers is fundamental to increasing the rubber's lifetime. So, modification by nanoparticles of rubbers and conventional rubbers composites has drawn substantial interest in research and industry due to the unique property profile achieved at low nanofiller content. Property enhancements will cover structural and functional properties of mechanical performance.

For longitudinal characteristics of aligned composites and nanotubes' mechanistic strengthening efficacy are higher than nanoplatelets with the same aspect ratio. For most random orientation cases and higher aspect ratios nanoparticles, nanoplatelets' geometric characteristics enable better strengthening; however, the same degree of dispersion and extinction in the same volume fraction. Depending upon the nanoparticular-polymer interaction, this difference will significantly affect the nanocomposites' bulk efficiency.

Macromolecules are rarely made of Rubber materials only due to them not having the most optimal performance. They are complex structures with several components, including elastomers and various additives with different functions. The desired output is obtained by multiple mechanical, thermal, optical, electrical and chemical properties [8]. The degree of strengthening by filler depends on several variables, of which a broad polymer-filler interface is the most significant development. Carbon blacks and silicas are the best known reinforcing fillers. There are extensively used silicates, clays, whiting (calcium carbonate), and other mineral fillers if there is no high reinforcement grade. Carbon blacks constitute the preeminent class in terms of tonnage and different properties of strengthening fillers. Incomplete combustion of hydrocarbons or thermal cracking is the preparation of carbon blacks. Currently, nearly all rubber carbon blacks are made with processes for the oil furnace. Oil or, more often, natural gas is cracked on a hot refractory surface in the thermal phase without oxygen. Besides carbon blacks for rubber applications, several grades are mainly developed for applications not using rubber [9].

Attract attention to the topological limitation principle refers to the strong interactions spontaneously formed by the contact with a soft material that conforms its components (i.e. chain segments) with a suitable area geometry (or topology). Applied with carbon black (CB)-filled rubber compounds, this term readily reflects adsorbing/desorbing balance of chain segments at suitable positions on CB aggregates for various steps, such as viscosity and modulus. This balance is reversed for both the magnitude of the strain or temperature or the two. To address rheological quantities directly linked to CB and rubber, relatively simple mathematical models can be created. Due to their experimental simplicity, the strain sweep (SS) test protocols with sufficient rheometers are ideal, as shown by tests on various CB-filled compounds and an adequate math modelling of results obtained when played at constant frequency strain amplitude and temperature [10].

For preparing natural rubber (NR) nanocomposites, multi-wall carbon nanotube (MWNTs) were used. The nanostructures in MWNTs/NR nanocomposites integrated carbon nanotubes into a polymer solution and evaporated the

solvent. Nanotubes can be distributed homogeneously into the NR matrix to improve their mechanical properties with this technology. The nanocomposites' properties, including tensile strength, tensile modulus, tear strength, break extension and hardness, have been investigated. The mechanical experiments show up to 12 times with purity of NR in the initial modulus. The dispersion status of the MWNTs into NR and mechanical inspection were explored better to understand the final device's morphology [11]. The elastomer materials are characterised by significant enough deformation or non-linear hyperelastic behaviour, which results in the formation, through the different orientations, of a slightly entangled network with weak interactions [12,13]. Rubber's mechanical properties are mainly determined by configurational entropic and molecular stretching. The rubber elasticity principle, invariant/stretch dependent continuum mechanics, and computational finite element analyses describe elastomers' non-linear hyperelastic behaviour [14,15].

Rubber is a highly complex material from the perspective of its actions. It is not easy to construct a component model that can predict the rubber's behaviour. Many researchers have worked on this for an extended period. Primarily, it was based on polynomial scale dynamics, the Ogden Model, the Mooney-Rivlin Model, and Yeoh [16-17]. Different models are used to quantify the stress-energy function. The decision is made depending on whether or not test data is available [18]. Finite element simulation provides good outcomes as Tensile test results from uniaxial, biaxial, and planar directions are applied. Uniaxial test evidence is insufficient when dynamic stresses perform better [19,20]. Different models are used to quantify the stress-energy function. The decision is made depending on whether or not test evidence is available [21,22]. Wei et al. [10] perform a finite element rubber analysis under high deformation. He also addressed the implementations of the finite element in the finite element. The predictive thermodynamic and continuum mechanics models are well-established for the hyperelastic material models.

The experimental technique for evaluating the constituent models, mathematical derivations, and disputes are discussed. Are performed on some experiments, including uniaxial, planar, and biaxial tension [23-25]. Youjian [15], and Mullins [18], the tyre performance of the component model is simulated using a finite element method in the tyre industry. Quick transient reactions can also be simulated using the FE protocol. Zhang et al. [19], a model of strain invariants existed, Rivlin and Saunders [20], later generalised. Gent and Thomas [21] look at different strain energy functions. Smith [22], Valanis and Landel [23], and Ogden [24] proposed the basic stress pattern.

In this research, natural rubber products have been improved with mechanical properties by using carbon nanotubes with different percentages of multi-walled carbon nanotube subjected to high tensile loading.

2. Experimental work and preparation of samples

In this work, carbon nanotubes have been filled into natural rubber. The preparation of nanocomposites was carried out using toluene as a solvent by a solvent casting process. The additional volumes of carbon nanotubes were 0.2%, 0.4%, 0.6%, 0.8% and 1% by 100 grammes of the overall weight. Later on, the nanocomposite rubber was tested experimentally. This experiment aims to apply a tensile force to the test sample until it ruptures and then pulls it through to defeat. During the tensile load application [26-31], the system calculates property and produces a stress/strain curve from which different values, such as the modulus of elasticity, can be calculated. The tensile measuring unit used in this analysis (see Fig. 1) has an electro-mechanical test system that regularly applies uniaxial loading to test specimens [32-39]. In terms of capabilities and implementations, it serves a broad role.
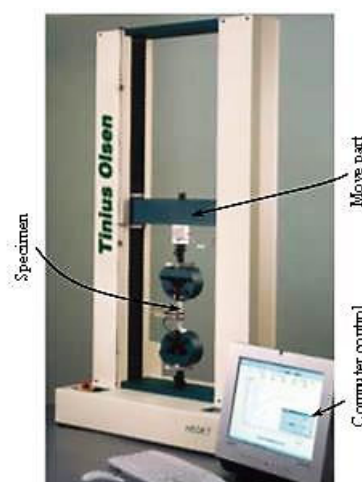
Fig. 1. Tensile test machine

The tensile machine performs load versus elongation (stress vs strain) measurements, which involves applying forces ranging from a few newtons to thousands of newtons, squeezing specimens with rubber grips, and calculating the resultant forces (stresses) and deformations (strains) [40-44]. Later, tensile force and strain sensors that produce an electrical transducer, a signal proportional to the applied stress or strain, are susceptible to measured loads and strains

[45-50]. This electric signal is digitised, weighed, and digitised again. Finally, this electrical signal is analysed, digitised, and then used to exhibit, study, and report tension, strain, and other approximate content parameters. The tensile tests for strength after stretching were conducted according to standards (D412-98), and the experiments were repeated five times, with the average effects being shown and checked each time [51-54].

The excellent capability of producing rubber nano-composites is proven by automobile tyres and other rubber materials, one of the most used and long-lasting groups of industrial items for more than a century. The exact meaning can be said for large-scale rubber compounding methods, Qusai et al. [55-58], which have been creating the nanocomposites found in tyres for almost a century, long before the word "nano" attracted academics' and engineers' attention. Many issues involve rubber nanocomposite mechanical behaviours for tensile loading. In general, the nanocomposite rubber applications are subjected to large tensile loading. So, the principles of large deformation rubber are fundamental in nano rubber applications.

Consequently, it is essential to create precise, reliable available models to understand rubber nanocomposites' behaviour better. The main challenge is the expectations under which a given theoretical model fails to predict significant deformation behaviour of elastomer nano-composites, as models are proposed for neat rubbers. More judgmentally, they can hardly be supposed to remain valid for systems in which four or more nanofillers having different nature, shapes, and sizes are used. This research attempts to use non-linear hyperelastic models for the non-linear tensile behaviour of rubbers for nanocomposites containing multi-walled carbon nanotubes (MWCNTs).

3. Strain energy

The energy potential stored by an object's deformation is called strain energy (Ogden et al. [59]). The straining energy is the same as creating regular and shear strains for a perfectly elastic material. The strain energy is restored when the stress-producing strain is eliminated. Complete recovery is achieved for a completely elastic material, and due to energy dissipation, the recovery is partial for plastic material. The strain energy is a function that connects a material strain to the energy that this deformation produces. The strain energy density (U), Strain Energy Density (SED), determined by unit body volume, is strain energy. SED is an excellent content indication since it is standardised to body height. The strain-energy function can be seen as a generalisation of the law of Hooke, which systematically defines complex elastic components [59].

3.1. Ogden form models

Ogden is [24] a designed model for large deformation isotropic elasticity. It is applied to characterise material's non-linear stress-stress behaviour, such as rubbers and polymers. Similar to other hyperelastic substance models. The Ogden model was built on the premise that the substance's action maybe by the strain's energy density function, which is isotropic, incompressible and isotope, Independent strain threshold. The general model of Ogden strain energy potential below Equation shows,

$$U = \sum_{i=1}^{N} \frac{2\mu_i}{\alpha_i^2}\left(\lambda_1^{\alpha i} + \lambda_2^{\alpha i} + \lambda_3^{\alpha i} - 3\right) \tag{1}$$

The Ogden model is commonly employed when the model is enough to reflect test data of up to 800% of the tensile test results. The Ogden paradigm is also a much more scalable description of the experiment's data than the other hyperelastic.

3.2. Neo-Hookean model

A model Neo-Hookean is analogous to the principle of Hooke and is suitable to simulate the material's non-linear stress tension behaviour under a wide variety of deformations. In 1948 Ronald Rivlin developed the model (Ericksen and Rivlin [60]). This model is based on the thermodynamics of crosslinked polymer chains used for plastic products rubber-like and 21. The initial stage of cross-connected polymer is neo-Hookean, and as tension is applied shift to each other. The shape of the Neo-Hookean strain energy potential is as follows,

$$U = C_{10}(I_1 - 3) + C_{01}(I_2 - 3) + \frac{1}{D_1}(J_{el} - 1) \tag{2}$$

3.3. Mooney-Rivlin model

Model Moony-Rivlin During the development of the original Mooney model, various observations were made on the strain energy mechanism for rubber, starting with: (1) The substance is uniform and free of hysteresis; (2). The substance is isotropic initially, and during the deformation, (3) the deformation occurs without any alteration of volume (Mooney, [16]). The linear shape of stress-energy is initially suggested by Mooney as,

$$U = C_{10}(I_1 - 3) + \frac{1}{D_1}(J_{el} - 1)^2 \tag{3}$$

Based on the linear relationship between stress and strain in primary shear, the Mooney-Rivlin model provides a slightly better match to some experimental rubber data than pure elastic models with appropriate C1 and C2 options (Mooney [16], Crocker et al. [61]). Initially formulated for

rubber, the Mooney-Rivlin material is also used today to denote general incompressible organic tissue. The more advanced Ogden substance model has been used to model rubber and biological materials with even higher strains. (Breslavsky et al. [62]).

3.4. Yeoh model

The hyperelastic Yeoh model is often a reduced polynomial shape in the third order, suited to describe almost isotropic rubber-style materials (Renaud et al. [63]). According to Ronald Rivlin, the energy density function of the strain invariant sequences 1, 2, and 3 can be used to define the elastic characteristics of rubber. The Yeoh model for incompressible rubber is merely a function of 1, and the strain energy's energy potential is given by,

$$U = \sum_{i=1}^{N} c_{io} \binom{n}{k} x^k a^{n-k} = \begin{pmatrix} \sum_{i=1}^{N} c_{io}(\bar{I}_1 - 3)^i + \\ \sum_{k=1}^{N} \frac{1}{D_k}(J-1)^{2k} \end{pmatrix} \quad (4)$$

3.5. Arruda-Boyce model

The hyperelastic model of Arruda-Boyce used for fitting tensile tests the potential for the energy strain of the form,

$$U = \mu \begin{pmatrix} \frac{1}{2}(I_1 - 3) + \frac{1}{20\lambda_m^2}(I_1^2 - 9) \\ + \frac{11}{1050\lambda_m^4}(I_1^3 - 27) + \\ \frac{19}{7000\lambda_m^6}(I_1^4 - 81) + \\ \frac{519}{673750\lambda_m^8}(I_1^5 - 243) \end{pmatrix} + \frac{1}{D}\left(\frac{J_{el}^2-1}{2} - \ln J_{el}\right) \quad (5)$$

These strain-energy functions have been applied to different strains in which the model is best suited. Since these models are built based on mathematical formation, critical parameters are often difficult to obtain. As seen briefly in the equations, a mixture of parameters is in some cases connected to the initial shear module. That directly affects precise, durable and unique evaluation and selection of material models for various circumstances in material parameters.

4. Experimental results and fitting tensile tests

To compare different material models, Abaqus has a hyperelastic curve fitting capability. To determine mechanical parameters, Abaqus uses stress-strain data from uniaxial tests. In Abaqus, each set of stress-strain data is converted into a strain energy equation. Abaqus' hyperelastic material curve fitting feature allows the researcher to compare material

models with each other. There are hyperelastic material models that have been assessed, as depicted in Figures 2-7. To compare different material models, Abaqus has a hyperelastic curve fitting capability. Abaqus relies on specified stress-nominal strain data when performing uniaxial tests.
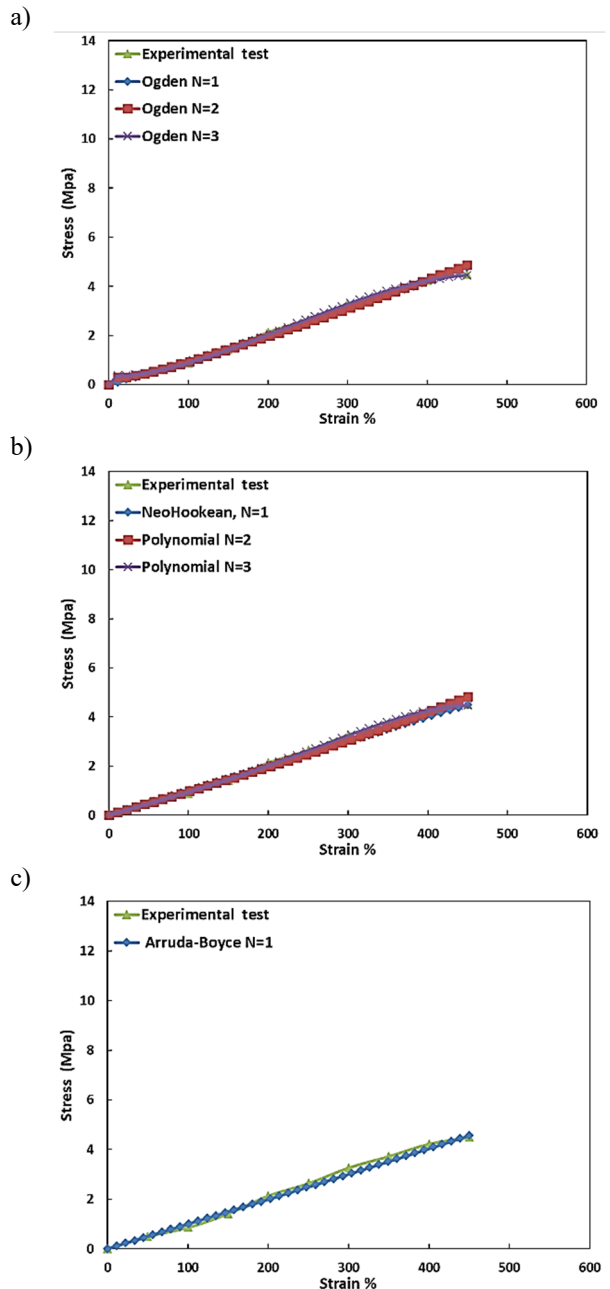

Fig. 2. Experimental and fitting of different hyperelastic models with tensile test rubber 0% multi-walled carbon nanotube; a) Ogden model N=1, 2, 3, b) Neo-Hookean N=1, Ploynomial N=2, 3, c) Arruda-Boyce N=1

a)

b)

c)

d)

Fig. 3. Experimental and fitting of different hyperelastic models with tensile test rubber 0.2% multi-walled carbon nanotube; a) Ogden model N=1, 2, b) Mooney-Rivelin model N=1, c) Neo-Hookean N=1, Ploynomial N=2, 3, d) Arruda-Boyce N=1

a)

b)

Fig. 4. Experimental and fitting of different hyperelastic models with tensile test rubber 0.4% multi-walled carbon nanotube; a) Ogden model N=1, 2, b) Mooney-Rivelin model N=1

Fig. 4. *cont.* Experimental and fitting of different hyperelastic models with tensile test rubber 0.4% multi-walled carbon nanotube; c) Neo-Hookean N=1, Ploynomial N=2, 3, d) Arruda-Boyce N=1
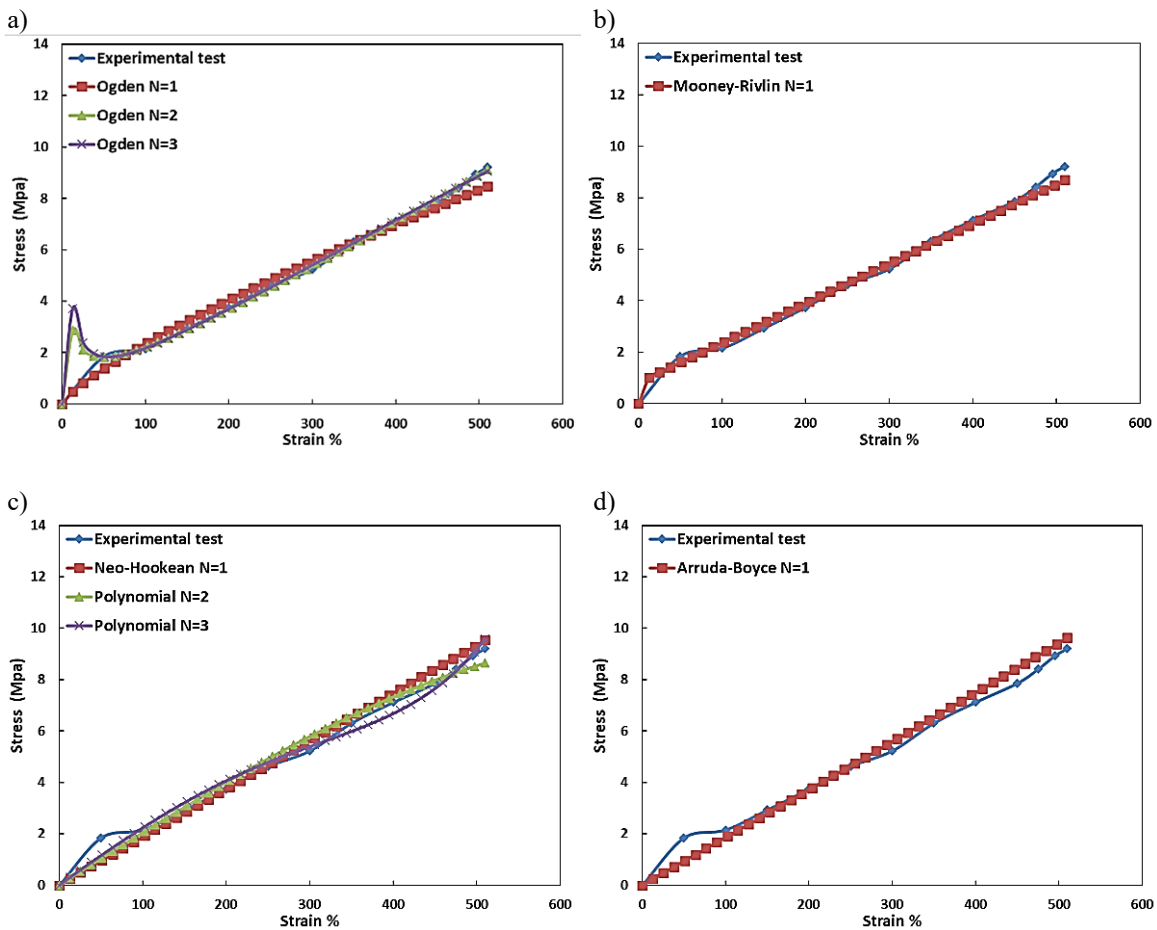
Fig. 5. Experimental and fitting of different hyperelastic models with tensile test rubber 0.6% multi-walled carbon nanotube; a) Ogden model N=1, 2, 3, b) Mooney-Rivelin model N=1, c) Neo-Hookean N=1, Ploynomial N=2, 3, d) Arruda-Boyce N=1
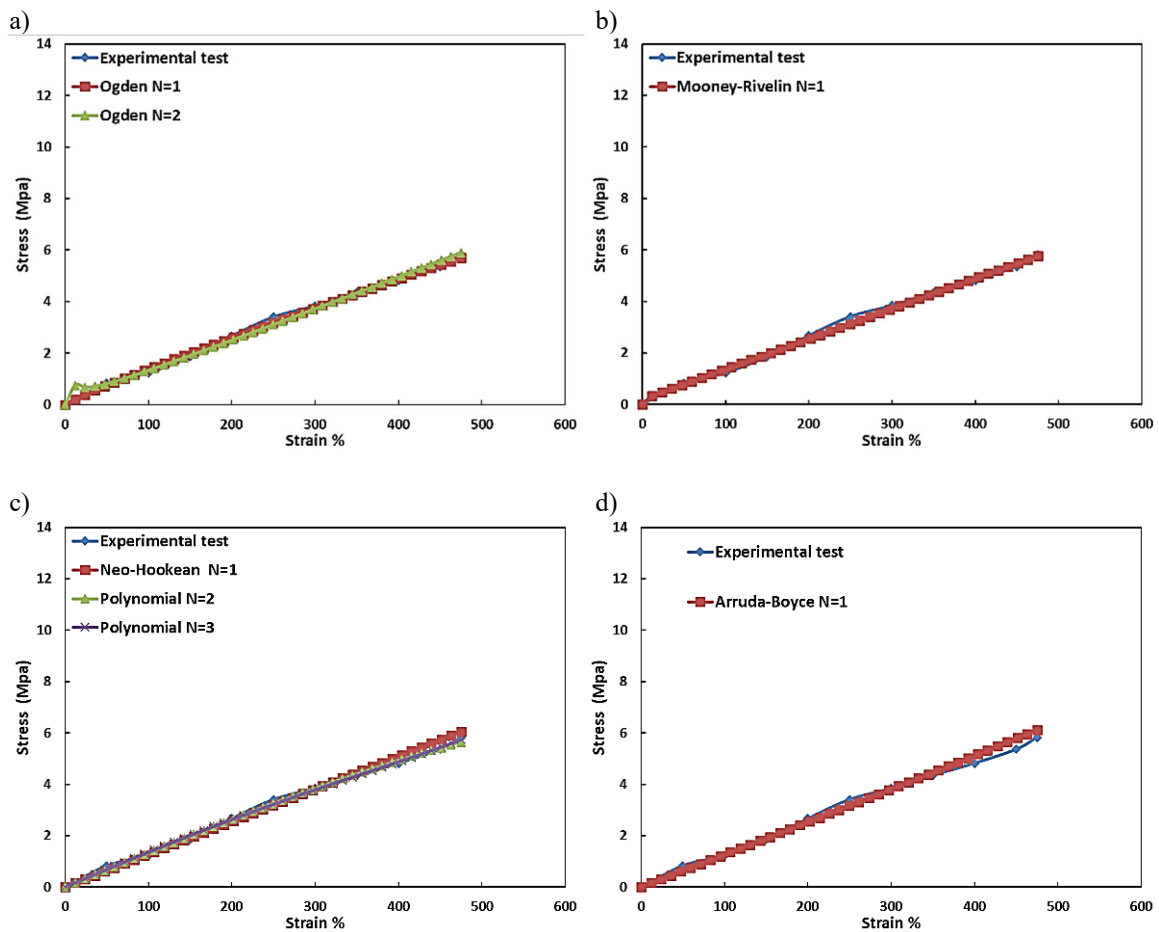
Fig. 6. Experimental and fitting of different hyperelastic models with tensile test rubber 0.8% multi-walled carbon nanotube; a) Ogden model N=1, 2, b) Mooney-Rivelin model N=1, c) Neo-Hookean N=1, Ploynomial N=2, 3, d) Arruda-Boyce N=1
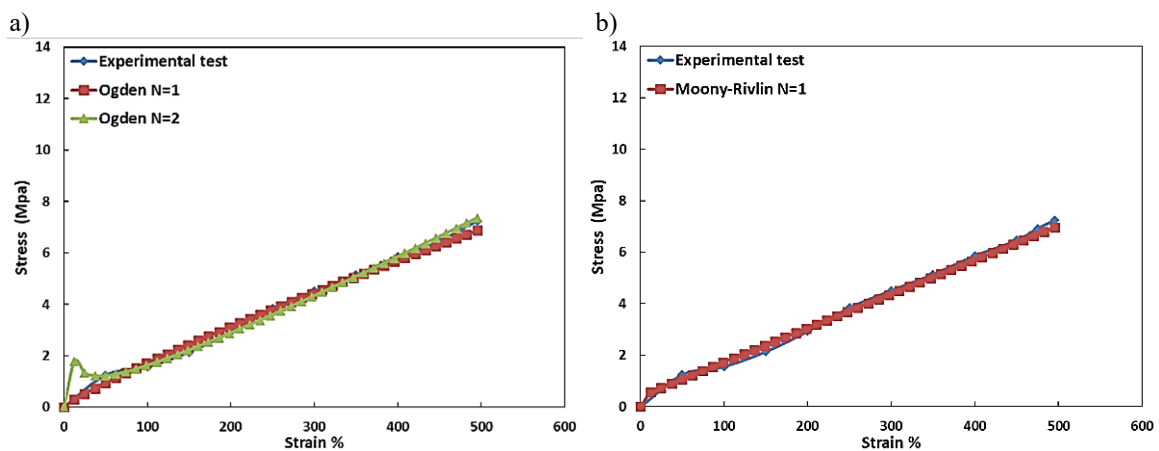

Fig. 7. Experimental and fitting of different hyperelastic models with tensile test rubber 1% multi-walled carbon nanotube; a) Ogden model N=1, 2, b) Mooney-Rivelin model
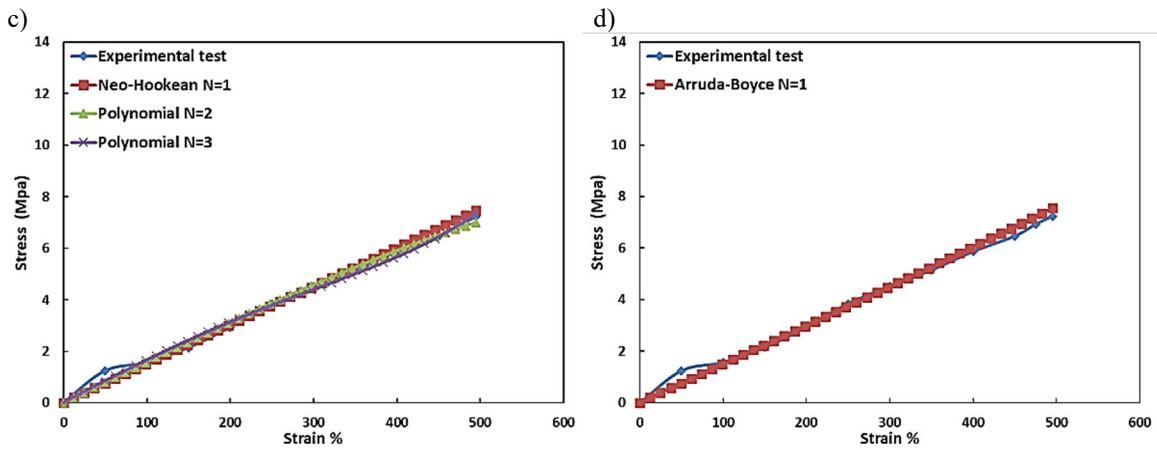
c)

d)

Fig. 7. *cont.* Experimental and fitting of different hyperelastic models with tensile test rubber 1% multi-walled carbon nanotube; c) Neo-Hookean N=1, Ploynomial N=2, 3, d) Arruda-Boyce N=1
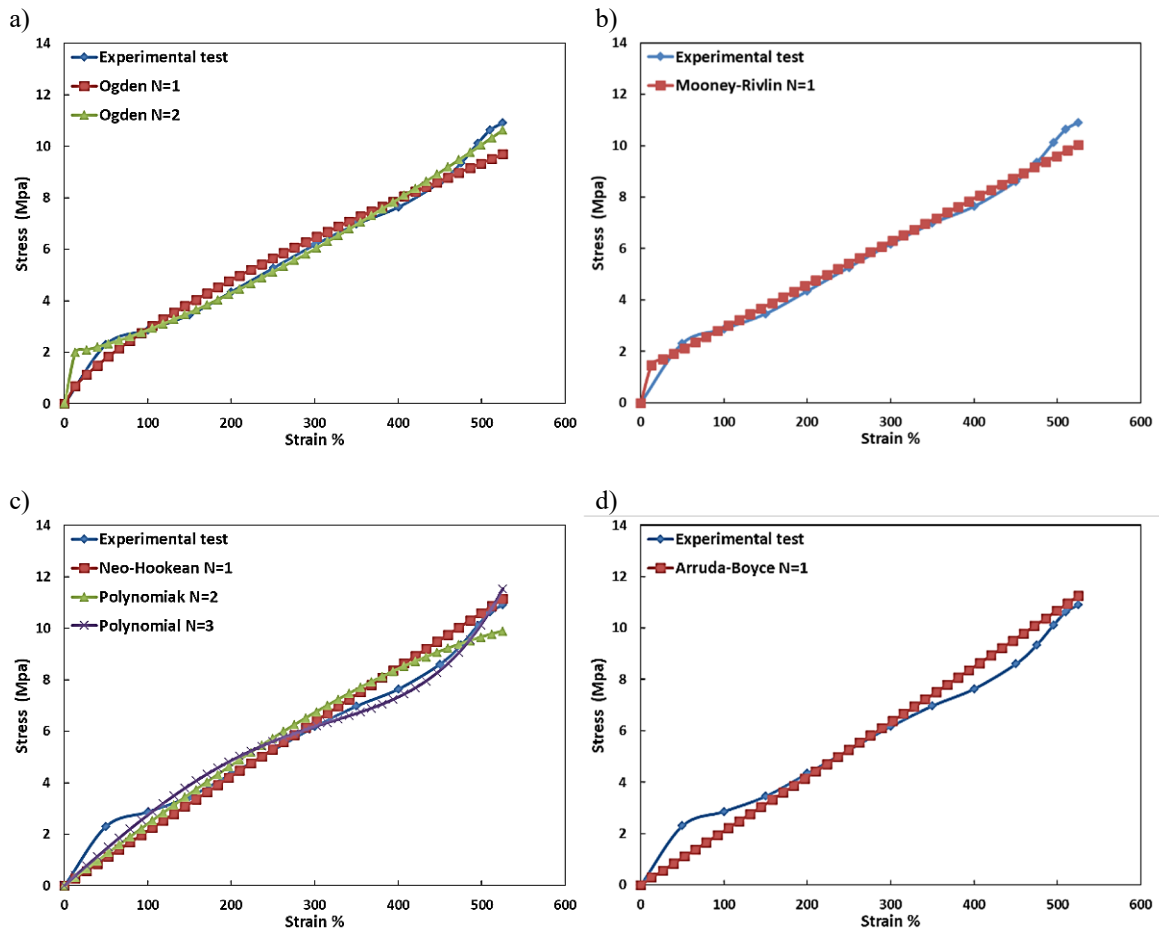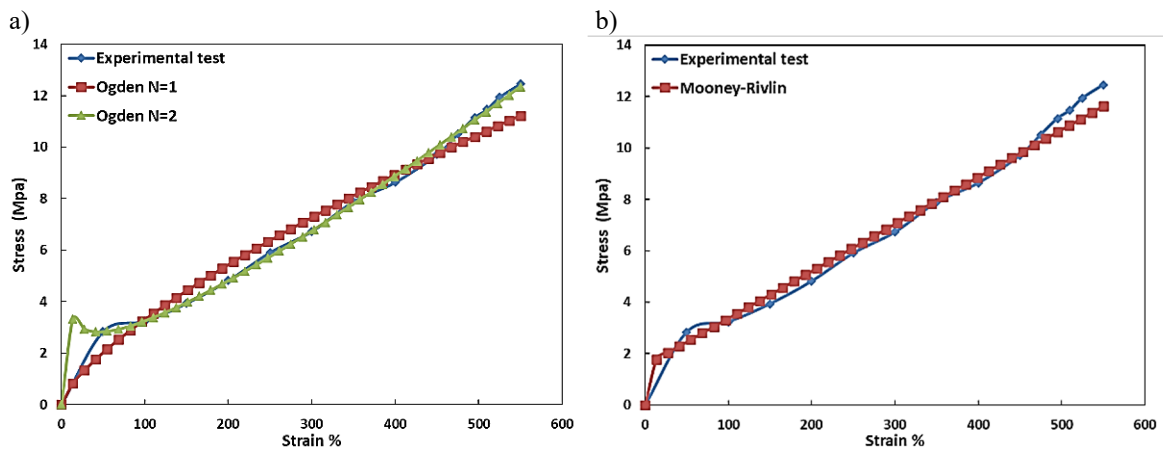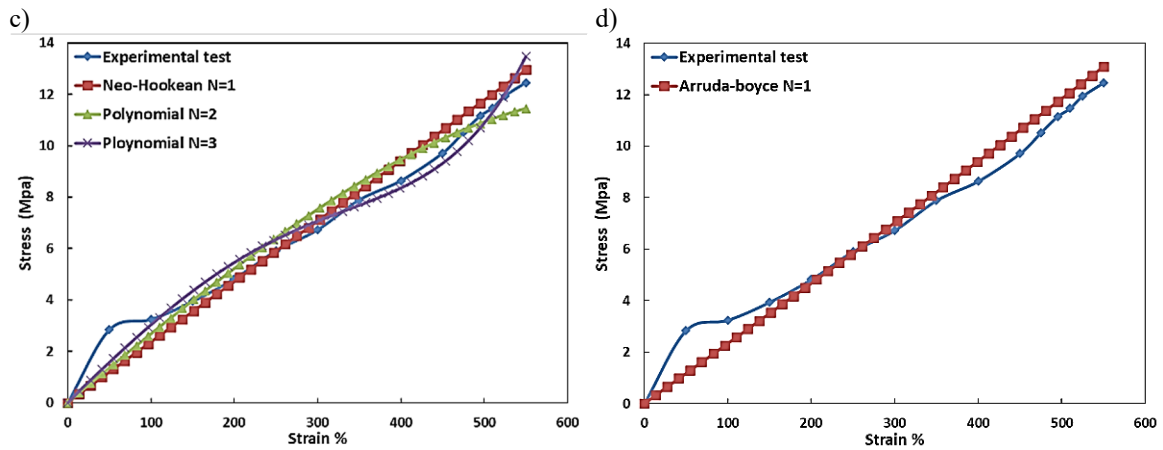
Table 1.
Material models used for material prediction parameters with 0% multi-walled carbon nanotube

Hyperelasticity model No 1: Ogden Model	Parameters						
	μ1	α1	μ2	α2	μ3	α3	Fitting error %
Ogden N=1	7.11E-03	2.07	-	-	-	-	3.32
Ogden N=2	5E-03	.136	0.39	-0.18			2.71
Ogden N=3	2.27E-04	2.79	-1.12E-07	4.00	0.40	-1.81	0.48

Hyperelasticity model No 2: Polynomial Model	Parameters							
	D1	C10	C01	D2	C20	C11	C02	Fitting error %
Polynomial (Mooney-Rivlin) N=1	-	-	-	-	-	-	-	Unstable
Polynomial N=2	-	-	-	-	--		-	Unstable

Hyperelasticity model No 3: Reduced Polynomial	Parameters										
	D1	C10	C01	D2	C20	C11	C02	C30	C21	C12 C03	Fitting error %
Neo-HookeN=1	0	4.99E-03	0	-	-	-	-	-	- D3	-	- -	5.34
N=2	0	4.77E-03	0	0	1.43E-09	0	0	-	-	-	- -	3.99
Yeoh N=3	0	4.48E-03	0	0	7.96E-09	0	0	0	-2.23E-14	0	0	1.85

Hyperelasticity model No 4: Arruda-Boyce	Parameters			
	μ	μo	λ	D Fitting error %
	9.90E-03	9.90E-03	1352.99	0 4.87

Hyperelastic models were the most accurate in predicting rubber formulation behaviour because they could match experimental data points at small and large strain values.

Mooney-Rivlin and Neo-Hookean coefficients and Arruda-Boyce and Ogden models calculated all deformation modes in Abaqus. Models like Ogden (N=2, N=3) were the

most accurate in predicting rubber formulation behaviour because they could match experimental data points at small and large strain values. Using the Mooney-Rivlin and Neo-Hookean coefficients and models from Arruda-Boyce, Absqus calculated all deformation modes for each test. Tables 1-6 show an unimportant parameter to a particular model. The mechanical properties were predicted using uniaxial tensile data to produce these results [55,56, 63-70]. The Ogden model N=3 has a fitting error of 0.48%, while the rest models predicted parameters with more significant fitting errors [71-75].

Table 2.
Material models used for material prediction parameters with 0.2% multi-walled carbon nanotube

	μ1	α1		μ2	α2	μ3		α3	Fitting error %
Ogden N=1	1.94E-02	1.91		-		-		-	4.16
Ogden N=2	1.06E-02	2.02		1.11	-0.18	-		-	2.34
Ogden N=3	-	-		-	-	-		-	Unstable

Hyperelasticity model No 2: Polynomial Model	D1	C10	C01	D2	C20	C11	C02	Fitting error %
Polynomial (Mooney-Rivlin) N=1	0	5.87e-3	9.27e-2					3.10
Polynomial N=2	-	-	-	-	-	-	-	Unstable

Hyperelasticity model No 3: Reduced Polynomial	D1	C10	C01	D2	C20	C11	C02	D3	C30	C21	C12	C03	Fitting error %
Neo-Hooke N=1	0	6.35e-2	0	-	-	-	-	-	-	-	-	-	7.14
N=2	0	6.70e-3	0	0	-1.73e-8	0	0	-	-	-	-	-	5.37
Yeoh N=3	0	6.18e-3	0	0	-3.52e-9	0	0	0	5.28e-15	0	0	0	5.24

Hyperelasticity model No 4: Arruda-Boyce	μ	μo	λ	D	Fitting error %
N=1	1.25e-2	1.25e-2	1428	0	7.8

Table 3.
Material models used for material prediction parameters with 0.4% multi-walled carbon nanotube

Hyperelasticity model No 1: Ogden Model	μ1	α1	D1	μ2	α2	D2	μ3	α3	Fitting error %
Ogden N=1	2.89e-2	1.87	0	-	-	-	-	-	9.57
Ogden N=2	8.06e3	2.10	0	3.10	-0.18	0	-	-	1.04
Ogden N=3	-	-	-	-	-	-	-	-	Unstable

Hyperelasticity model No 2: Polynomial Model	D1	C10	C01	D2	C20	C11	C02	Fitting error %
Polynomial (Mooney-Rivlin) N=1								
Polynomial N=2	0	3	0	0		0		14.05

Table 3. *cont.*

Hyperelasticity model No 3:	Parameters												
Reduced Polynomial	D1	C10	C01	D2	C20	C11	C02	D3	C30	C21	C12	C03	Fitting error %
Neo-Hooke N=1	0	7.51e-3	0	-	-	-	-	-	-	-	-	-	15.75
N=2	0	7.91e-	0	0	-1.77e-9	0	-	-	-	-	-	-	14.05
Yeoh N=3	0	8.35e-3	0	0	-7.95e-09	0	0	0	1.64E-14	0	0	0	12.85

Hyperelasticity model No 4: Arruda-Boyce	Parameters					
	μ	μ_o	λ		Fitting error %	
N=1	1.48E-02	1.41E-02	1488		16.48	

Table 4.

Material models used for material prediction parameters with 0.6% multi-walled carbon nanotube

Hyperelasticity model No 1: Ogden Model	Parameters						
	μ_1	α_1	μ_2	α_2	μ_3	α_3	Fitting error %
Ogden N=1	5.44E-02	1.79	-	-	-	-	11.29
Ogden N=2	1.23E-02	2.06155759	5.17196953	-0.18	-	-	0.34
Ogden N=3	14.77	-0.29	4.29E-2	-3.93	-7.48	-0.97	0.27

Hyperelasticity model No 2: Polynomial Model	Parameters							
	D1	C10	C01	D2	C20	C11	C02	Fitting error %
Polynomial (Mooney-Rivlin) N=1	0	7.71E-03	0.40	-	-	-	-	4.44
Polynomial N=2	-	-	-	-	-	-	-	Unstable

Hyperelasticity model No 3:	Parameters												
Reduced Polynomial	D1	C10	C01	D2	C20	C11	C02	D3	C30	C21	C12	C03	Fitting error %
Neo-Hooke N=1	0	9.32E-03	0	-	-	-	-	-	-	-	-	-	27.02
N=2	0	1.02E-02	0	0	-3.40E-09	0	0	-	-	-	-	-	22.19
Yeoh N=3	0	1.14E-02	0	0	-1.89E-08	0		0	3.81E-14	0	0		16.71

Hyperelasticity model No 4: Arruda-Boyce	Parameters			
	μ	μ_o	λ	Fitting error %
N=1	1.84E-2	1.84E-2	1533	28.24

Table 5.

Material models used for material prediction parameters with 0.8% multi-walled carbon nanotube

Hyperelasticity model No 1: Ogden Model	Parameters						
	μ_1	α_1	μ_2	α_2	μ_3	α_3	Fitting error %
Ogden N=1	-0.18	1.72	-	-	-	-	12.48
Ogden N=2	2.12E-03	2.35	1.93	-1.99	-		0.81
Ogden N=3	-	-	-	-	-	-	Unstable

Table 5. *cont.*

Hyperelasticity model No 2: Polynomial Model	Parameters							
	D1	C10	C01	D2	C20	C11	C02	Fitting error %
Polynomial (Mooney-Rivlin) N=1	0	8.368E-3	0.61	-	-	-	-	0.40
Polynomial N=2	-	-	-	-	-	-	-	Unstable

Hyperelasticity model No 3: Reduced Polynomial	Parameters												
	D1	C10	C01	D2	C20	C11	C02	D3	C30	C21	C12	C03	Fitting error %
Neo-Hooke N=1	0	1.05E-02	0	-	-	-	-	-	-	-	-	-	39.25
N=2	0	1.20E-02	0	0	-4.75E-09	0	0	-	-	-	-	-	30.93
Yeoh N=3	0	1.42E-02	0	0	-2.95E-08	0	0		5.70E-14	0	0	0	18.89

Hyperelasticity model No 4: Arruda-Boyce	Parameters			
	μ	μo	λ	Fitting error %
N=1	2.092E-02	2.09E-02	1578.00	40.83

Table 6.

Material models used for material prediction parameters with 1% multi-walled carbon nanotube

Hyperelasticity model No 1: Ogden Model	Parameters						
	$\mu1$	$\alpha1$	$\mu2$	$\alpha2$	$\mu3$	$\alpha3$	Fitting error %
Ogden N=1	0.10	1.719	-	-	-	-	15.78
Ogden N=2	6.65E-03	2.19	5.09	-1.37	-	-	0.38
Ogden N=3							Unstable

Hyperelasticity model No 2: Polynomial Model	Parameters							
	D1	C10	C01	D2	C20	C11	C02	Fitting error %
Polynomial (Mooney-Rivlin) N=1	0	9.17E-03	0.75	-	-	-	-	5.27
Polynomial N=2	-	-	-	-	-	-	-	Unstable

Hyperelasticity model No 3: Reduced Polynomial	Parameters												
	D1	C10	C01	D2	C20	C11	C02	D3	C30	C21	C12	C03	Fitting error %
Neo-Hooke N=1	0	1.17E-02	0	-	-	-	-	-	-	-	-	-	44.82
N=2	0	1.33E-02	0	0	-4.95E-09	0	0	-	-	-	-	-	35.95
Yeoh N=3	0	1.56E-02	0	0	-2.80E-08	0	0	0	4.92E-14	0	0	0	25.28

Hyperelasticity model No 4: Arruda-Boyce	Parameters			
	μ	μo	λ	Fitting error %
N=1	2.32E-02	2.32E-02	1653.00	46.45

5. Conclusions

Young's modulus and Poisson's ratio can describe the linear elastic material behaviour. The behaviour of hyperelastic materials is more complicated, as complex strain energy functions can only describe it, making it more challenging to evaluate and model this category. The tensile testing method for natural rubber filled with a multi-wall carbon nanotube is studied, including testing configurations. Theoretical foundations and current research on Abaqus software FE modelling methods and optimisation programmes have been formed.

This paper aims to review the hyperelastic properties of nanocomposite rubber. In practice, no reliable rules are available for stress-strain testing behaviour. The most stable and acceptable options are the models N=1, and N=2 of Ogden, in ABAQUS, in FEM. The models were tested. Tensile loading of nanocomposite rubber examined by Yeoh and Arruda-Boyce offers a solid analysis of the material response and a stable analysis. The numerical and experimental findings are reconciled. Regression analysis is used to determine the relationship.

List of symbols

U	Strain energy density
λ_i $(i = 1,2,3)$	Stretch ratio
μ_i	Material constant related to the initial shear modulus
α_i	Empirically calculated material constants
λ_U	The stretch ratio in the principal direction
ε_i	Principal nominal strain
σ_U	Tensile stress
E	Relative error
E_k	Vector of relative errors
P_{ik}	A derivative of the vector of relative errors
N	Order of the polynomial
n	Number of data points
σ_i^{th}	Initial theoretical stress
σ_i^{exp}	Initial experimental stress
δ_{ij}	Degree of deformation
σ_k^{th}	Total theoretical stress
γ	Shear strain
c	Material constant
λ	Extensions of the deformation
r	Iteration count
R	Relative root mean square error

References

[1] L. Bokobza, O. Rapoport, Reinforcement of natural rubber, Journal of Applied Polymer Science 85/11 (2002) 2301-2316.
DOI: https://doi.org/10.1002/app.10858

[2] A. Amin, Constitutive Modeling for Strain-Rate Dependency of Natural and High Damping Rubbers, Saitama University, Research Report, Saitama, 2001.

[3] A. Amin, A. Lion, S. Sekita, Y. Okui, Non-linear dependence of viscosity in modeling the rate-dependent response of natural and high damping rubbers in compression and shear: experimental identification and numerical verification, International Journal of Plasticity 22/9 (2006) 1610-1657.
DOI: https://doi.org/10.1016/j.ijplas.2005.09.005

[4] T.A. Vilgis, G. Heinrich, M. Klüppel, Reinforcement of Polymer Nano-Composites: Theory, Experiments and Applications, Cambridge University Press, Cambridge, 2009.
DOI: https://doi.org/10.1017/CBO9780511605314

[5] F. Laraba-Abbes, P. Ienny, R. Piques, A new 'Tailor-made' methodology for the mechanical behaviour analysis of rubber-like materials: II. Application to the hyperelastic behaviour characterisation of a carbon-black filled natural rubber vulcanizate, Polymer 44/3 (2003) 821-840. DOI: https://doi.org/10.1016/S0032-3861(02)00719-X

[6] A. Khodadadi, G. Liaghat, H. Ahmadi, A.R. Bahramian, Y. Anani, O. Razmkhah, S. Asemeni, Numerical and experimental study of impact on hyperelastic rubber panels, Iranian Polymer Journal 28/2 (2019) 113-122.
DOI: https://doi.org/10.1007/s13726-018-0682-x

[7] M. Shahzad, A. Kamran, M.Z. Siddiqui, M. Farhan, Mechanical characterisation and F.E. modelling of a hyperelastic material, Materials Research 18/5 (2015) 918-924.
DOI: https://doi.org/10.1590/1516-1439.320414

[8] L.R.G. Treloar, The elasticity of a network of long-chain molecules – III, Transactions of the Faraday Society 42/1 (1946) 83-94.
DOI: https://doi.org/10.1039/TF9464200083

[9] E.M. Arruda, M.C. Boyce, A three-dimensional constitutive model for the large stretch behavior of rubber elastic materials, Journal of the Mechanics and Physics of Solids 41/2 (1993) 389-412. DOI: https://doi.org/10.1016/0022-5096(93)90013-6

[10] Y.T. Wei, T.Q. Yang, X.W. Du, The large deformation rubber-like materials: constitutive laws and finite element method, Acta Mechanica Solida Sinica - Chinese Edition 20/4 (1999) 281-289.

[11] A.N. Gent, A new constitutive relation for rubber, Rubber Chemistry and Technology 69/1 (1996) 59-61. DOI: https://doi.org/10.5254/1.3538357

[12] M. Al-Waily, I.Q. Al Saffar, S.G. Hussein, M.A. Al-Shammari, Life Enhancement of Partial Removable Denture made by Biomaterials Reinforced by Graphene Nanoplates and Hydroxyapatite with the Aid of Artificial Neural Network, Journal of Mechanical Engineering Research and Developments 43/6 (2020) 269-285.

[13] M. Al-Waily, M.H. Tolephih, M.J. Jweeg, Fatigue Characterization for Composite Materials used in Artificial Socket Prostheses with the Adding of Nanoparticles, IOP Conference Series: Materials Science and Engineering 928 (2020) 022107. DOI: https://doi.org/10.1088/1757-899X/928/2/022107

[14] N.D. Fahad, A.A. Kadhim, R.H. Al-Khayat, M. Al-Waily, Effect of SiO_2 and Al_2O_3 hybrid nano materials on fatigue behavior for laminated composite materials used to manufacture artificial socket prostheses, Materials Science Forum 1039 (2021) 493-509. DOI: https://doi.org/10.4028/www.scientific.net/MSF.1039.493

[15] M.W. Youjian, Elastomer test used by the hyperelastic material model in finite element analysis, Special Purpose Rubber Product 22/5 (2001) 52-55.

[16] M. Mooney, A theory of large elastic deformation, Journal of Applied Physics 11/9 (1940) 582-592. DOI: https://doi.org/10.1063/1.1712836

[17] O.H. Yeoh, Some forms of the strain energy for rubber, Rubber Chemistry and Technology 66/5 (1993) 754–771. DOI: https://doi.org/10.5254/1.3538343

[18] L. Mullins, Effect of stretching on the properties of rubber, Rubber Chemistry and Technology 21/2 (1948) 281-300. DOI: https://doi.org/10.5254/1.3546914

[19] Z.G. Zhang, M.J. Zheng, J.L. Xie, Research on Finite Element Emulation of Temporal Impetus Response on Resilient Wheel, Journal of Beijing Jiaotong University 27/1 (2003) 25-27.

[20] R.S. Rivlin, D.W. Saunders, Large elastic deformations of isotropic materials VII. Experiments on the deformation of rubber, Philosophical Transactions of the Royal Society A 243/865 (1951) 251-288. DOI: https://doi.org/10.1098/rsta.1951.0004

[21] A.N. Gent, A.G. Thomas, Forms for the stored (strain) energy function for vulcanised rubber, Journal of Polymer Science 28/118 (1958) 625-628. DOI: https://doi.org/10.1002/pol.1958.1202811814

[22] L.J. Hart-Smith, Elasticity parameters for finite deformations of rubber-like materials, Journal of Applied Mathematics and Physics (ZAMP) 17 (1966) 608-626. DOI: https://doi.org/10.1007/BF01597242

[23] K.C. Valanis, R.F. Landel, The strain-energy function of a hyperelastic material in terms of the extension ratios, Journal of Applied Physics 38 (1967) 2997. DOI: https://doi.org/10.1063/1.1710039

[24] R.W. Ogden, Large deformation isotropic elasticity-on the correlation of theory and experiment for incompressible rubber-like solids, Proceedings of the Royal Society A 326/1567 (1972) 565-584. DOI: https://doi.org/10.1098/rspa.1972.0026

[25] A.K. Abdulameer, M.A. Al-Shammari, Fatigue Analysis of Syme's Prosthesis, International Review of Mechanical Engineering (IREME) 12/3 (2018) 293-301. DOI: https://doi.org/10.15866/ireme.v12i3.14390

[26] J.S. Chiad, M. Al-Waily, M.A. Al-Shammari, Buckling Investigation of Isotropic Composite Plate Reinforced by Different Types of Powders, International Journal of Mechanical Engineering and Technology 9/9 (2018) 305-317.

[27] S.G. Hussein, M.A. Al-Shammari, A.M. Takhakh, M. Al-Waily, Effect of Heat Treatment on Mechanical and Vibration Properties for 6061 and 2024 Aluminum Alloys, Journal of Mechanical Engineering Research and Developments 43/1 (2020) 48-66.

[28] E.N. Abbas, M.J. Jweeg, M. Al-Waily, Fatigue Characterization of Laminated Composites used in Prosthetic Sockets Manufacturing, Journal of Mechanical Engineering Research and Developments 43/5 (2020) 384-399.

[29] F.M. Kadhim, A.M. Takhakh, J.S. Chiad, Modeling and Evaluation of Smart Economic Transfemral Prosthetic, Defect and Diffusion Forum 398 (2020) 48-53. DOI: https://doi.org/10.4028/www.scientific.net/DDF.398.48

[30] M. Al-Waily, M.A. Al-Shammari, M.J. Jweeg, An Analytical Investigation of Thermal Buckling Behavior of Composite Plates Reinforced by Carbon Nano Particles, Engineering Journal 24/3 (2020) 11-21. DOI: https://doi.org/10.4186/ej.2020.24.3.11

[31] A.H. Jeryo, J.S. Chiad, W.S. Abbod, Boosting Mechanical Properties of Orthoses-Foot Ankle by

Adding Carbon Nanotube Particles, Materials Science Forum 1039 (2021) 518-536. DOI: https://doi.org/10.4028/www.scientific.net/MSF.1039.518

[32] M.A. Al-Shammari, M. Al-Waily, Theoretical and Numerical Vibration Investigation Study of Orthotropic Hyper Composite Plate Structure, International Journal of Mechanical and Mechatronics Engineering 14/6 (2014) 1-21.

[33] S.M. Abbas, A.M. Takhakh, M.A. Al-Shammari, M. Al-Waily, Manufacturing and Analysis of Ankle Disarticulation Prosthetic Socket (SYMES), International Journal of Mechanical Engineering and Technology 9/7 (2018) 560-569.

[34] E.E. Kader, A.M. Abed, M.A. Al-Shammari, Al_2O_3 Reinforcement Effect on Structural Properties of Epoxy Polysulfide Copolymer, Journal of Mechanical Engineering Research and Developments 43/4 (2020) 320-328.

[35] S.A. Mechi, M. Al-Waily, Impact and Mechanical Properties Modifying for Below Knee Prosthesis Socket Laminations by using Natural Kenaf Fiber, Journal of Physics: Conference Series 1973 (2021) 012168.
DOI: https://doi.org/10.1088/1742-6596/1973/1/012168

[36] M. Al-Waily, A.M. Jaafar, Energy balance modelling of high velocity impact effect on composite plate structures, Archives of Materials Science and Engineering 111/1 (2021) 14-33.
DOI: https://doi.org/10.5604/01.3001.0015.5562

[37] A.M. Obaid, J.S. Chiad, G.Sh. Sadiq, Incremental Forming of AA8006 Aluminum Alloys Sheet with Different Step Size, Materials Science Forum 1039 (2021) 137-143. DOI:
https://doi.org/10.4028/www.scientific.net/MSF.1039.137

[38] S.A. Mechi, M. Al-Waily, A. Al-Khatat, The Mechanical Properties of the Lower Limb Socket Material Using Natural Fibers: A Review, Materials Science Forum 1039 (2021) 473-492. DOI:
https://doi.org/10.4028/www.scientific.net/MSF.1039.473

[39] E.K. Njim, S.H. Bakhy, M. Al-Waily, Analytical and Numerical Investigation of Free Vibration Behavior for Sandwich Plate with Functionally Graded Porous Metal Core, Pertanika Journal of Science and Technology 29/3 (2021) 1655-1682.
DOI: https://doi.org/10.47836/pjst.29.3.39

[40] M.A. Al-Shammari, M. Al-Waily, Analytical Investigation of Buckling Behavior of Honeycombs Sandwich Combined Plate Structure, International Journal of Mechanical and Production Engineering Research and Development 8/4 (2018) 803-818. DOI: https://doi.org/10.24247/ijmperdaug201883

[41] E.N. Abbas, M. Al-Waily, T.M. Hammza, M.J. Jweeg, An investigation to the effects of impact strength on laminated notched composites used in prosthetic sockets manufacturing, IOP Conference Series: Materials Science and Engineering 928 (2020) 022081. DOI: https://doi.org/10.1088/1757-899X/928/2/022081

[42] E.K. Njim, S.H. Bakhy, M. Al-Waily, Analytical and numerical free vibration analysis of porous functionally graded materials (FGPMs) sandwich plate using Rayleigh-Ritz method, Archives of Materials Science and Engineering 110/1 (2021) 27-41. DOI: https://doi.org/10.5604/01.3001.0015.3593

[43] A.A. Kadhim, E.A. Abbod, A.K. Muhammad, K.K. Resan, M. Al-Waily, Manufacturing and Analyzing of a New Prosthetic Shank with Adapters by 3D Printer, Journal of Mechanical Engineering Research and Developments 44/3 (2021) 383-391.

[44] M. Al-Waily, M.J. Jweeg, M.A. Al-Shammari, K.K. Resan, A.M. Takhakh, Improvement of Buckling Behavior of Composite Plates Reinforced with Hybrids Nanomaterials Additives, Materials Science Forum 1039 (2021) 23-41. DOI:
https://doi.org/10.4028/www.scientific.net/MSF.1039.23

[45] M.A. Al-Shammari, S.E. Abdullah, Stiffness to Weight Ratio of Various Mechanical and Thermal Loaded Hyper Composite Plate Structures, IOP Conference Series: Materials Science and Engineering 433 (2018) 012051.
DOI: https://doi.org/10.1088/1757-899X/433/1/012051

[46] Y.A. Shafeeq, J.S. Chiad, Y.Y. Kahtan, Study, analysis, the vibration and stability for the artificial hand during its daily working, International Journal of Mechanical Engineering and Technology 9/13 (2018) 1706-1716.

[47] M.A. Al-Shammari, Q.H. Bader, M. Al-Waily, A.M. Hasson, Fatigue Behavior of Steel Beam Coated with Nanoparticles under High Temperature, Journal of Mechanical Engineering Research and Developments 43/4 (2020) 287-298.

[48] S.H. Bakhy, M. Al-Waily, M.A. Al-Shammari, Analytical and numerical investigation of the free vibration of functionally graded materials sandwich beams, Archives of Materials Science and Engineering 110/2 (2021) 72-85.
DOI: https://doi.org/10.5604/01.3001.0015.4314

[49] M.J. Jweeg, K.I. Mohammed, M.H. Tolephih, M. Al-Waily, Investigation into the Distribution of Erosion-Corrosion in the Furnace Tubes of Oil Refineries,

Materials Science Forum 1039 (2021) 165-181. DOI: https://doi.org/10.4028/www.scientific.net/MSF.1039.165

[50] F.T. Al-Maliky, J.S. Chiad, Study and evaluation of four bar polycentric knee used in the prosthetic limb for transfemoral amputee during the gait cycle, Materials Today: Proceedings 42/5 (2021) 2706-2712. DOI: https://doi.org/10.1016/j.matpr.2020.12.709

[51] M.A. Al-Shammari, Experimental and FEA of the Crack Effects in a Vibrated Sandwich Plate, Journal of Engineering and Applied Sciences 13/17 (2018) 7395-7400.

[52] M.A. Husain, M.A. Al-Shammari, Analytical Solution of Free Vibration Characteristics of Partially Circumferential Cracked Cylindrical Shell, Journal of Mechanical Engineering Research and Developments 43/3 (2020) 442-454.

[53] E.K. Njim, S.H. Bakhy, M. Al-Waily, Optimisation Design of Functionally Graded Sandwich Plate with Porous Metal Core for Buckling Characterisations, Pertanika Journal of Science and Technology 29/4 (2021) 3113-3141. DOI: https://doi.org/10.47836/pjst.29.4.47

[54] E.K. Njim, S.H. Bakhy, M. Al-Waily, Analytical and Numerical Investigation of Buckling Behavior of Functionally Graded Sandwich Plate with Porous Core, Journal of Applied Science and Engineering 25/2 (2022) 339-347. DOI: https://doi.org/10.6180/jase.202204_25(2).0010

[55] Q.H. Jebur, M.J. Jweeg, M. Al-Waily, H.Y. Ahmad, K.K. Resan, Hyperelastic models for the description and simulation of rubber subjected to large tensile loading, Archives of Materials Science and Engineering 108/2 (2021) 75-85. DOI: https://doi.org/10.5604/01.3001.0015.0256

[56] Q.H. Jebur, M.J. Jweeg, M. Al-Waily, Ogden model for characterising and simulation of PPHR rubber under different strain rates, Australian Journal of Mechanical Engineering (2021) (published online). DOI: https://doi.org/10.1080/14484846.2021.1918375

[57] Q.H. Jebur, P. Harrison, Z. Guo, G. Schubert, X. Ju, V. Navez, Characterisation and modelling of a transversely isotropic melt-extruded low-density polyethylene closed cell foam under uniaxial compression, Proceedings of the Institution of Mechanical Engineers, Part C: Journal of Mechanical Engineering Science 226/9 (2012) 2168-2177. DOI: https://doi.org/10.1177/0954406211431528

[58] Q.H. Jebur, P. Harrrison, Z. Guo, G. Schubert, V. Navez, Characterisation and modelling of a melt-extruded LDPE closed cell foam, Applied Mechanics

and Materials 70 (2011) 105-110. DOI: https://doi.org/10.4028/www.scientific.net/AMM.70.105

[59] R.W. Ogden, G. Saccomandi, I. Sgura, Fitting hyperelastic models to experimental data, Computational Mechanics 34 (2004) 484-502. DOI: https://doi.org/10.1007/s00466-004-0593-y

[60] J.L. Ericksen, R.S. Rivlin, Large Elastic Deformations of Homogeneous Anisotropic Materials, Journal of Rational Mechanics and Analysis 3/3 (1954) 281-301.

[61] L.E. Crocker, B.C. Duncan, J.M. Urquhart, R.G. Hughes, A. Olusanya, The application of rubber material models to analyse flexible adhesive joints, National Physical Laboratory, Teddington, 2011.

[62] I.D. Breslavsky, M. Amabili, M. Legrand, Nonlinear vibrations of thin hyperelastic plates, Journal of Sound and Vibration 333/19 (2014) 4668-4681. DOI: https://doi.org/10.1016/j.jsv.2014.04.028

[63] F. Renaud, J.L. Dion, G. Chevallier, I. Tawfiq, R. Lemaire, A new identification method of viscoelastic behaviour: Application to the generalised Maxwell model, Mechanical Systems and Signal Processing 25/3 (2011) 991-1010. DOI: https://doi.org/10.1016/j.ymssp.2010.09.002

[64] M.M. Abdulridha, N.D. Fahad, M. Al-Waily, K.K. Resan, Rubber Creep Behavior Investigation with Multi-Wall Tube Carbon Nano Particle Material Effect, International Journal of Mechanical Engineering and Technology 9/12 (2018) 729-746.

[65] M. Al-Baghdadi, M.J. Jweeg, M. Al-Waily, Analytical and Numerical Investigations of Mechanical Vibration in the Vertical Direction of a Human Body in a Driving Vehicle using Biomechanical Vibration Model, Pertanika Journal of Science & Technology 29/4 (2021) 2791-2810. DOI: https://doi.org/10.47836/pjst.29.4.30

[66] T.S.N. Aswad, M.A.R.S. Al-Baghdadi, M. Al-Waily, M.A.B. Razali, Performance Enhancement of a Photovoltaic Cell Working in Hot Environment Conditions using Al_2O_3 Nanofluids: A CFD Study, International Journal of Nanoelectronics and Materials 14/4 (2021) 317-328.

[67] E.K. Njim, S.H. Bakhy, M. Al-Waily, Free vibration analysis of imperfect functionally graded sandwich plates: analytical and experimental investigation, Archives of Materials Science and Engineering 111/2 (2021) 49-65. DOI: https://doi.org/10.5604/01.3001.0015.5805

[68] M.J. Jweeg, Z.Kh. Hamdan, A.H. Majeed, K.K. Resan, M. Al-Waily, A new method for measurement the residual stresses in friction stir welding, Archives of

Materials Science and Engineering 112/2 (2021) 63-69. DOI: https://doi.org/10.5604/01.3001.0015.6287

[69] M.A. Al-Shammari, M.A. Husain, M. Al-Waily, Free Vibration Analysis of Rectangular Plates with Cracked Holes, AIP Conference Proceedings 2386 (2022) 040023. DOI: https://doi.org/10.1063/5.0066908

[70] E.K. Njim, S.H. Bakhy, M. Al-Waily, Analytical and numerical flexural properties of polymeric porous functionally graded (PFGM) sandwich beams, Journal of Achievements in Materials and Manufacturing Engineering 110/1 (2022) 5-15. DOI: https://doi.org/10.5604/01.3001.0015.7026

[71] S.M.J. Haider, A.M. Takhakh, M. Al-Waily, A Review Study on Measurement and Evaluation of Prosthesis Testing Platform during Gait Cycle within Sagittal Plane, 14th International Conference on Developments in eSystems Engineering "DeSE", Sharjah, United Arab Emirates, 2021, 223-228. DOI: https://doi.org/10.1109/DeSE54285.2021.9719575

[72] S.M.J. Haider, A.M. Takhakh, M. Al-Waily, Y. Saadi, Simulation of gait cycle in sagittal plane for above-knee prosthesis, AIP Conference Proceedings 2386 (2022) 040002. DOI: https://doi.org/10.1063/5.0066819

[73] Z.A.A. Abud Ali, A.M. Takhakh, M. Al-Waily, A review of use of nanoparticle additives in lubricants to improve its tribological properties, Materials Today: Proceedings 52/3 (2022) 1442-1450. DOI: https://doi.org/10.1016/j.matpr.2021.11.193

[74] R.H. Al-Khayat, A.A. Kadhim, M.A.R.S. Al-Baghdadi, M. Al-Waily, Flow parameters effect on water hammer stability in hydraulic system by using state-space method, Open Engineering 12/1 (2022) 215-226. DOI: https://doi.org/10.1515/eng-2022-0014

[75] R.H. Al-Khayat, A.W.A. Al-Fatlawi, M.A.R.S. Al-Baghdadi, M. Al-Waily, Water hammer phenomenon in pumping stations: A stability investigation based on root locus, Open Engineering 12/1 (2022) 254-262. DOI: https://doi.org/10.1515/eng-2022-0029